Nucleation kinetics, optical, dielectric, piezoelectric and NLO properties of KADP (85:15) mixed crystals

G. IYAPPAN, P. RAJESH*, P. RAMASAMY
Department of Physics, SSN College of Engineering, Kalavakkam, Tamil Nadu, India

In the present work, mixed crystals of KADP (85:15) have been grown at 45 ºC using solution growth. The growth parameters such as solubility, metastable zone width and induction period are determined experimentally. Nucleation parameters such as critical radius, interfacial tension and critical free energy of the mixed crystals are calculated. The UV-Visible spectrum shows that the mixed crystal has good optical transmission in the entire visible and near IR region. The dielectric measurements are used to analyse dielectric constant and dielectric loss of the mixed crystal. The nonlinear optical property of the grown crystal has been confirmed by the Kurtz powder technique and second harmonic generation efficiency is found to be 1.5 times that of potassium dihydrogen phosphate (KDP) crystal. Photoconductivity study shows the positive photo conducting nature of the crystal. Higher piezoelectric coefficient has been observed in mixed crystals.

(Received July 16, 2018; accepted April 8, 2019)

Keywords: Solubility, Solution growth, NLO materials

1. Introduction

In recent years, the development of new nonlinear optical mixed crystals has attained wide interests for electro optical modulation and frequency conversion. The materials such as ADP and KDP have been extensively studied for their fruitful NLO applications [1-4]. The ADP and KDP materials have high standard scale in NLO applications [2]. Srinivasan et.al, have grown mixed crystals of ADP and KDP with different compositions using slow evaporation technique and reported their compositional dependence of morphology, micro hardness and optical properties [5,6]. Similarly, Shenoy et al., have investigated the formation of mixed crystals of ADP and KDP with different molar ratio and their thermal properties [7]. Xiue Ren et al., reported the fundamental growth behaviours of KDP, ADP and mixed crystals (KADP) both experimentally and theoretically [8]. Fabrico Mendes souza et al., reported the electrical conductivity in ADP, KDP mixed crystals [9]. Srinivasan et al., and De-Gao et al., [6] reported the non-availability of crystals from all the compositions and a large mismatch in lattice constants between the systems. Rajesh et al., [10] analysed the growth rate and other parameters of the mixed crystals grown with 90:10 ratio.

Even though, there are no report on nucleation kinetics parameters and no bulk size crystals are shown with intermediate compositions such as 85:15, 80:20. The present work reports the solubility at different temperatures. The induction period, which changes inversely proportional to the nucleation rate has been used to determine the interfacial tension between the KADP and aqueous solution. By using interfacial tension, the nucleation parameters such as Gibbs free energy change for the formation of critical nucleus, ΔG^*, free energy of formation, ΔG, radius of the nucleus, r and number of molecules in the critical nucleus, i* have been calculated [11]. In addition to that, SHG efficiency, piezoelectric nature of the crystals and various optical properties such as transmittance, photoconductivity, and optical band gap of the crystals are analysed.

2. Experimental

2.1. Solubility studies

GR grade KH_2PO_4 (KDP), GR grade $NH4H_2PO_4$ (ADP), and deionized water with 18.2 MΩ-cm resistivity were used. The experiment was carried out in 200 ml flat bottomed conical flask containing 100 ml deionized water at predefined temperatures kept inside a thermo stated water bath with a temperature control better than ±0.01 ºC. The solution was stirred continuously for an hour to achieve stabilization using an immiscible magnetic stirrer. Solubility was determined by gravimetric analysis for different temperatures (25-50 ºC) and the solubility curve is shown in Fig. 1. Comparing the results with the pure KDP, it was found that the mixing of ADP has increased the solubility of the pure KDP [12]. This may be due to the higher solubility of ADP.

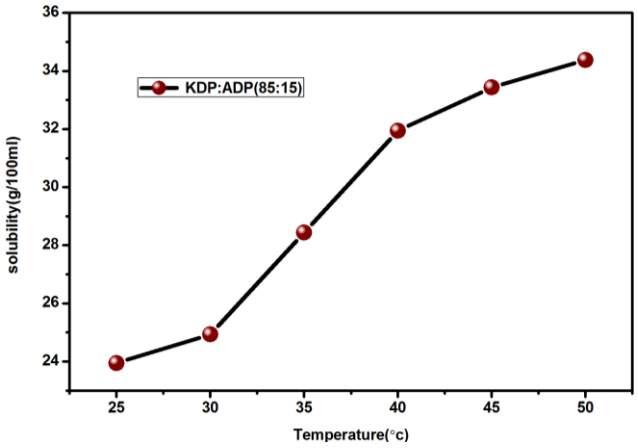

Fig. 1. Solubility curve of KADP mixed crystal

2.2. Determination of metastable Zone width

The stability of the growth solution with wide metastable zone width is important for the growth of bulk crystals. It depends on a number of factors such as stirring rate, cooling rate of the solution and the presence of additional impurities [13]. Using the solubility data, the saturated solution of KADP (85:15) was prepared. Nucleation studies were carried out with a constant temperature bath attached with a cryostat setup for six different temperatures such as 25, 30, 35, 40, 45, and 50ºC as per conventional polythermal method [14]. The saturated solution has been cooled to the nucleation temperature where the critical (first speck) nucleus has been identified. The difference between nucleation temperature and the saturation temperature was taken as a metastable zone width. For growing good quality crystals, wider metastable zone width is preferred. The solubility and nucleation curves are shown in Fig. 2.

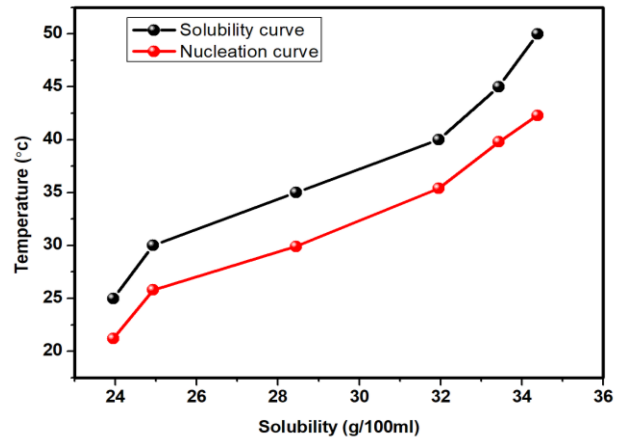

Fig. 2. Solubility and metastable zone width of KADP mixed crystal

2.3. Induction period measurements

This experiment was performed at selected degrees of super saturation (s), viz 1.05, 1.06, 1.07, 1.08 and 1.09 at constant temperature at 40ºC using isothermal method [15-16]. The required level of supersaturation was achieved by dissolving the required amount of KADP (85:15) in DI water. The solution was used to conduct induction period analysis. The appearance of first speck of the nucleus was seen at the bottom of the container and the time taken for the formation of the first crystal (primary nucleation) was measured and the same procedure has been repeated for different supersaturation ratios. The observed values are plotted and shown in Fig. 3. It indicates that the induction period of mixed KADP (85:15) is less than that of pure KDP. The presence of ADP in KDP affects the nucleation phenomena considerably. The plot of ln τ against $1/ (\ln S)^2$ is shown in Fig. 4.

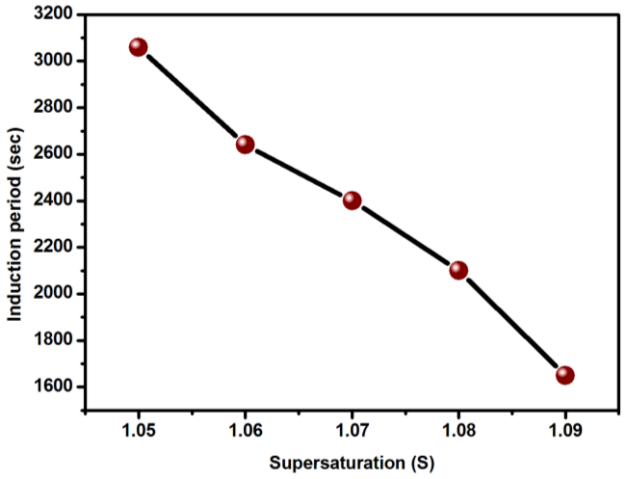

Fig. 3. Induction period vs Supersaturation ratio

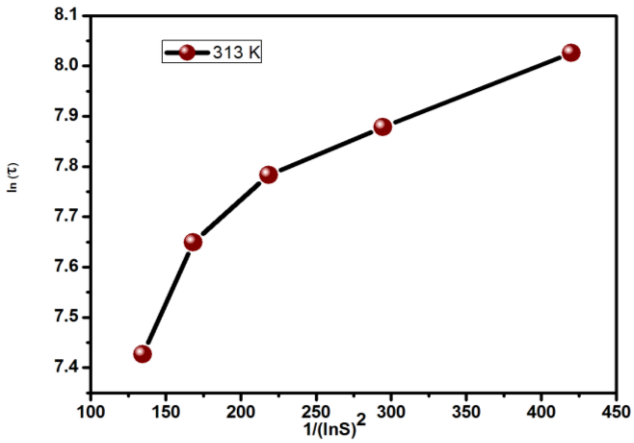

Fig. 4. ln (τ) vs $(lnS)^{-2}$ of KADP (85:15)

2.4. Nucleation kinetics theory of KDP: ADP (85:15)

The nucleation depends on the thermodynamic driving force, which in turn depends on the super saturation, temperature and impurities present in system [17]. The change in the Gibbs free energy (ΔG) between the crystalline phase and surrounding mother liquor results in a driving force which stimulates crystallization [18]. The free energy required to form a spherical nucleus is given by eqn. (1).

$$\Delta G = \frac{4}{3}\pi r^3 \Delta G_v + \pi 4 r^2 \gamma \tag{1}$$

where, ΔG_V is the energy change per unit volume and r is the radius of the nucleus. Using the classical theory of nucleation the volume excess free energy is calculated using eqn. (2).

$$\Delta G_v = -\Delta\mu / V \tag{2}$$

where, $\Delta\mu = kT \ln S$,V is the molecular volume, T is the particular saturation temperature, S is supersaturation ratio and k is the Boltzmann constant.

At the critical state, the free energy of formation obeys the condition d (ΔG)/dr = 0. Hence the radius of the critical nucleus with respect to supersaturation is expressed using eqn. (3)

$$r^* = -2\gamma / \Delta G_v \tag{3}$$

The interfacial tension is calculated using the experimental data and the theoretical expression 4 is used for homogeneous formation of spherical nuclei [19].

$$\ln \tau = \ln B + \left(\frac{16\pi\gamma^3}{3R^3T^3(\ln S)^2} \right) \tag{4}$$

where $\gamma^3 = \frac{3R^3T^3m}{16\pi V^2 N_A^3}$, R is gas constant, N_A is Avogadro's number, *ln B* depends on temperature.

$$\Delta G^* = 16\gamma^3 / 3(\Delta G_v)^2$$

The number of molecules in the critical nucleus is expressed using eqn. (5).

$$i^* = \frac{4\pi(r^*)^3}{3V} \tag{5}$$

where, i^* is number of molecules in the critical nucleus, r^* is radius of critical nucleus and V is molecular volume.

Also the critical radius (r_c) and Gibbs free energy for the formation of critical nucleus (ΔG_c) can be expressed using eqns. 6 & 7 respectively. The critical radius as a function of supersaturation is shown in Fig. 5.

$$r_c = \frac{2\gamma v}{kT \ln S} \tag{6}$$

$$\Delta G_c = \frac{4}{3}\pi\gamma r_c^2 = \frac{16\pi\gamma^3 v^2}{3k^2T^2 \ln^2 S} \tag{7}$$

where, ΔG_c is critical energy barrier, γ is the interfacial surface energy, k is the Boltzmann constant, T is the particular saturation temperature and S is a saturation ratio. The values were evaluated based on the above equations and it is given in Table 1. It is inferred from the Table 1 that, as the supersaturation is increased, the radius of critical nucleus (r_c) and the critical energy barrier (ΔG_c) decrease. Decrease in the critical radii value from 5.5643 to 3.1500 nm for mixed crystal occurs in the supersaturation range of 1.05 to 1.09. The time for the formation of critical nucleus increases with the decreases of supersaturation. Increase in time may lead to spurious nucleation. From the induction period measurements, the interfacial tension of KADP has been calculated from 25 ºC to 50ºC in steps of 5ºC. It is observed from the results that, the interfacial energy is directly related to the solubility and inversely propositional to the growth rate [13]. At 40ºC, the lowest supersaturation point S=1.05 produces no nucleation up to 3,060 seconds, whereas, the supersaturation point S=1.09, forms nucleation at 1,680 seconds itself. It is seen from the results that the induction period decreases with increase in supersaturation as expected from the classical nucleation theory [20].

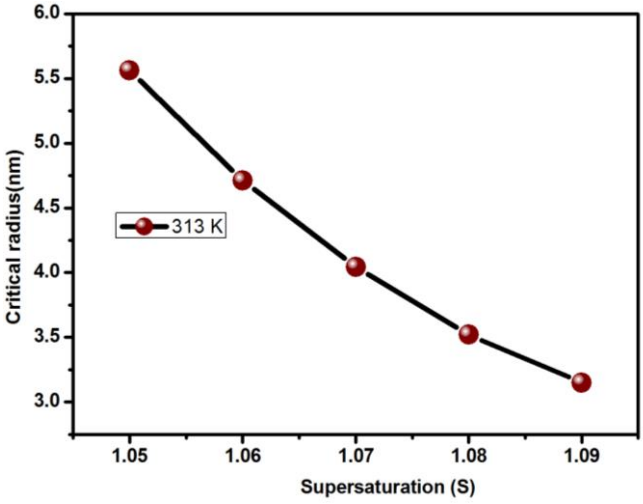

Fig. 5. Critical radius as a function of super saturation

Table 1. Nucleation Kinetics parameter of KADP mixed crystal at 313

S	τ (s)	$\Delta G_v \times 10^6$ (J/m^3)	$\Delta G^* \times 10^{-19}$	r* (nm)	i^*
1.05	3060	-0.6097	6.6617	5.5643	2091.6
1.06	2640	-0.7261	4.6545	4.7112	1269.55
1.07	2400	-0.8388	3.4876	4.0445	802.83
1.08	2100	-0.9635	2.6432	3.5211	525.56
1.09	1680	-1.0770	2.1155	3.1500	379.47

2.5. Crystal growth

The growth process was carried out in a constant temperature bath with an accuracy of ± 0.01 °C. In order to increase the purity the raw materials have been recrystallized. After successive recrystallization, the mixed crystal was grown using slow evaporation solution growth technique at 45 °C. The crystals were harvested in a span of 20 days. The sizes of the grown crystals are up to 10×10×10 mm^3. The grown crystal is shown in Fig. 6.

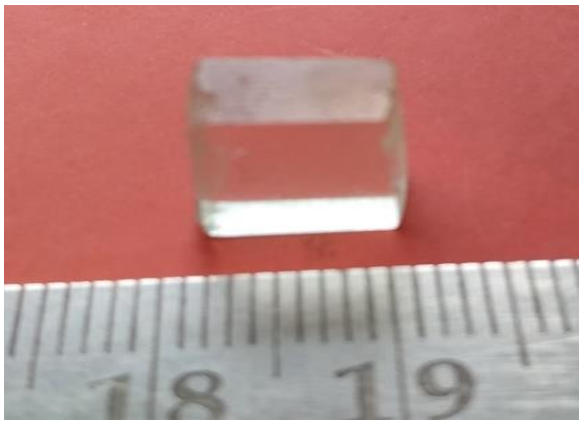

Fig. 6. KADP (85-15) mixed crystal

3. Etching studies of KADP (85:15)

Dislocations play an influential role in the crystal growth and have particular relationship in regard to their burgers vector with the crystal surface [21]. The quality of the grown crystal can be assessed by knowing the defect content and dislocations using chemical etching studies. Therefore the surface features were analyzed and examined using DI water as an etchant at room temperature using optical microscope in the reflection mode. The (100) face of the crystals free from the visible inclusions or micro cracks were selected for the studies. The Millipore water was used for etching study. The etch pits of the KADP were observed for different etching period 5 sec and 10 sec and it is shown in Fig. 7 a and b. Initially, the KADP crystal was dipped in Millipore water and then the surface was scrubbed gently using the tissue paper [22]. The rectangular hillock patterns were seen. It was observed that the morphology of etch pits strongly depends on the nature of the etchant and its crystal structure. It is inferred from the figures that when the etching time is increased, the size of the pits are also increased. The hillocks with symmetrical shape are the result of internal structural symmetries of the crystal [13]. The calculated etch-pit density is $3\times10^4/cm^2$ which indicates the good quality of the grown crystal.

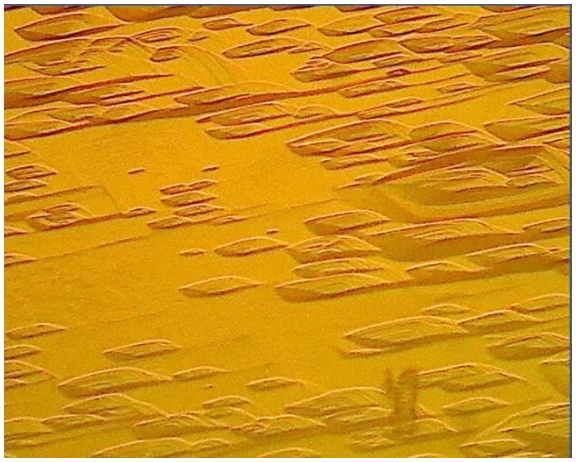

a)

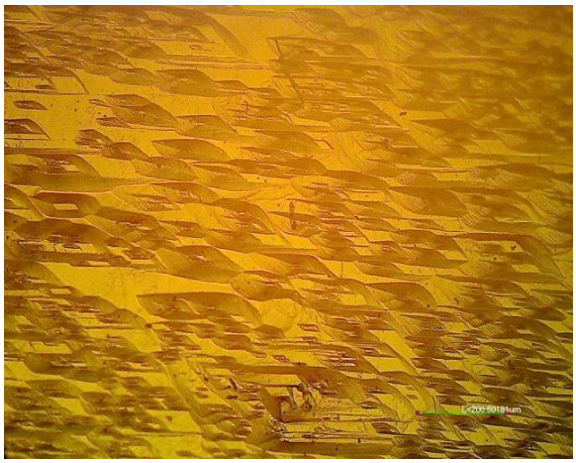

b)

Fig. 7. Surface of grown crystal after water etchant for (a) 5 s and (b) 10 s

4. UV-Vis spectral studies

Optical transmission studies were carriedout in the wavelength region from 200 to 1100 nm using Perkin-Elmer Lamda 35 UV-Vis spectrometer. The recorded spectrum is shown in Fig. 8. It is observed from the spectrum that the mixed crystal has nearly 80% of transmission in the entire visible region which is an important requirement for the NLO applications. In order to confirm the reproducibility, the experiments were repeated several times and the consistent results were observed. The optical band gap (E_g) estimated from the optical absorption coefficient (a) near the absorption edge for the indirect transition [23] is given by eqn. 8. The absorption coefficient was calculated from the transmission spectrum using the eqn. 9.

$$\alpha h\upsilon = A(h\upsilon - E_g)^{\frac{1}{2}} \tag{8}$$

where, E_g is the optical band gap of the crystal, A is the constant, v is the frequency of the incident light.

$$\alpha = \frac{2.3026}{t} \log_{10}\left(\frac{100}{T}\right) \quad (9)$$

where, T is the transmittance (%) and t is the thickness of grown mixed crystal.

The direct optical band gap of the grown mixed crystal was calculated by the plotting $(\alpha h\upsilon)^2$ versus $(h\upsilon)$ and is depicted in Fig. 9. The calculated bandgap is 5.3 eV. This difference in the electronic structure seems to be primarily important for the appearance of optical non linearity in the mixed crystal [24].

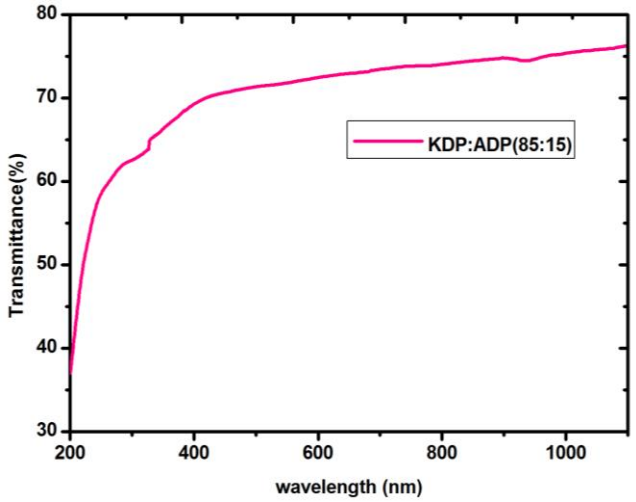

Fig. 8. UV-Vis-NIR spectra of KADP mixed crystal

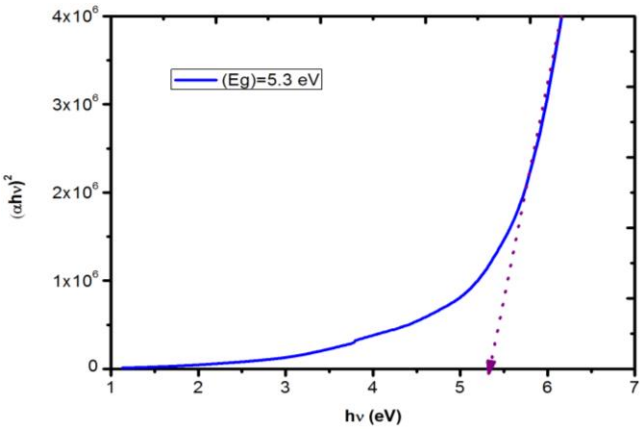

Fig. 9. Band gap energy graph of KADP mixed crystal

5. Dielectric measurements

The measurement of dielectric loss and dielectric constant has been done as a function of frequency at various temperatures using Agilent 428A LCR meter. The grown mixed crystal is coated with silver paste on both sides to act as a parallel plate capacitor. The capacitance of the crystal was measured at frequencies range from 1 kHz – 1 MHz. The dielectric constant of the mixed crystal [25] was calculated using the eqn. 10.

$$\varepsilon_r = C_{crys} / C_{air} \quad (10)$$

where, C_{crys} is the capacitance of the crystal and C_{air} is the capacitance of the air. Fig. 10 a and b shows the temperature dependence of the dielectric constant and dielectric loss of the grown mixed crystal. It is observed from the figure that the dielectric constant increases with increase in temperature and decreases with increase in frequency. It is also inferred that the grown mixed crystal's high dielectric constant and low dielectric loss compared to the pure ADP and KDP crystal indicates that the grown crystals are of good quality.

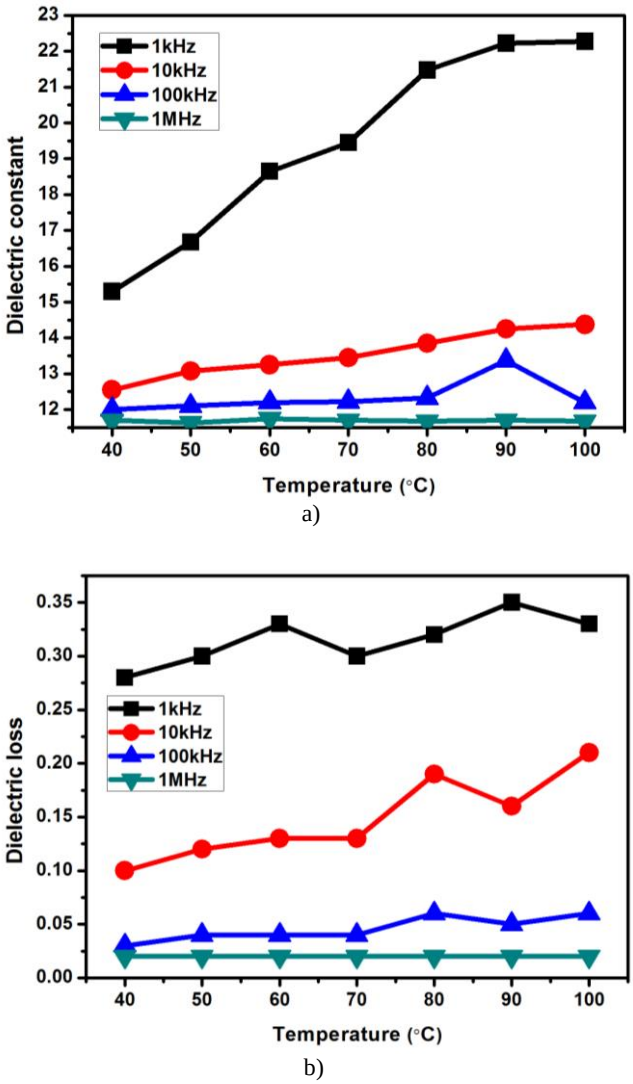

Fig. 10. (a) The temperature dependence of dielectric constant (b) The dielectric loss of KADP mixed crystal

6. SHG measurement

Qualitative measurement of the conversion efficiency of the crystal was determined using the powder technique developed by Perry and Kurtz. Q-switched Nd:YAG laser delivering input beam energy of 1.2mJ/pulse at the wavelength of 1064 nm with repetition rate of 10Hz and pulse width of 10 ns was used for this analysis. The uniformly powdered samples are tightly packed in the microcapillary tubes and illuminated using polarized laser beam. The bright green light at the output of the subjected samples confirms the prominent generation of SHG signals. The corresponding output voltages were recorded for KDP and the KADP crystals. KDP was used as a reference material in the SHG measurement. The observed values of the grown mixed crystal and the reference material are given in the Table 2. It is evident from the studies that the SHG conversion efficiency is 1.5 times that of the pure KDP. The presence of ADP and better crystalline perfection may be the reasons for the increase in SHG efficiency. Molecular alignment through inclusion complexation can also be the reason for the increase of SHG efficiency [26].

Table 2. SHG efficiency of grown KADP mixed crystal

S.no	Crystal	SHG efficiency
1	Pure ADP	30mV
2	Pure KDP	18mV
3	KADP(85:15)	23 mV

7. Photoconductivity studies

Photoconductivity measurement was carried out on the polished portion of the grown mixed crystal. The two electrodes of thin copper wire of 0.3 mm thickness were fixed using silver paint and the sample was connected in series with a DC power supply and KEITHLEY 485 picoammeter. The dark current and the photocurrent of the grown mixed crystal were measured as a function of voltage and are shown in Fig. 11. It was observed that the photoconductivity of the crystal increased with the increasing voltage. Linear increase in the dark current and photocurrent with the applied voltage was also noted from the study. It is evident that the photocurrent is always greater than the dark current and hence the grown mixed crystal has positive photoconductivity. This may be due to the generation of mobile charge carriers by the absorption of photons [27-28].

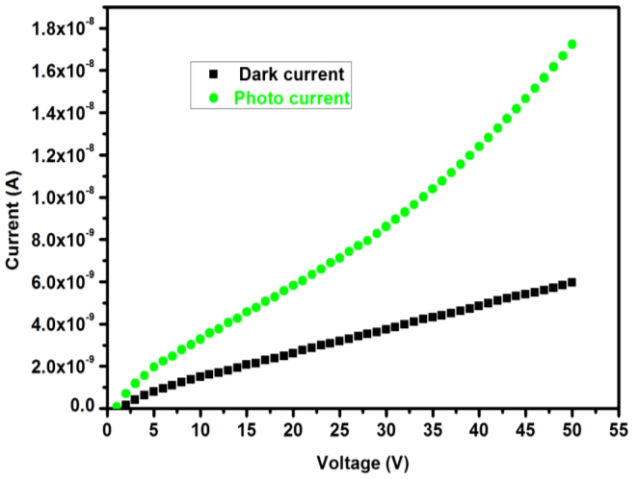

Fig. 11. Photoconductivity spectrum of KADP mixed crystal

8. Piezoelectric studies

The Piezoelectric study was performed using SINOCERA (YE2730A d_{33} METER). The grown mixed crystal is poled at 0.5 kV/cm for 1 hour at room temperature. Piezoelectric materials are those which produce electric charge when a mechanical force is applied on them or conversely develop strain under the application of the electric field. In either way, there is a linear coupling between stress and the applied field. Owing to it, the piezoelectric coefficient value (d_{33}) obtained for the grown mixed crystal was 5 pC/N which is higher compared to the pure systems. The values are given in the Table 3. This may be due to the presence of ADP in the KDP lattice and leads to creation of large dipoles on the application of mechanical stress.

Table 3. Piezoelectric charge coefficient (d_{33}) values of the KADP mixed crystal

S.no.	Crystal	Piezoelectric charge coefficient(d_{33}) value (pC/N)
1	ADP[10]	0.12
2	KDP[10]	0.04
3	KADP(85:15)	0.24

9. Conclusion

The good quality of KADP (85:15) mixed crystal has been grown successfully using slow evaporation solution using DI water as solvent. Solubility of KADP is increased due to addition of ADP. The interfacial tensions are calculated based on induction period values. 80% of transmission has been recorded in the entire visible region shows the suitability of the crystals for device fabrication. The SHG conversion efficiency of KADP crystal is higher than pure KDP. The Photoconductivity studies show that

grown crystal exhibits positive photoconductive nature. Higher piezoelectric values indicate the suitability of the crystal for various device applications. It is concluded that the present work will be useful to grow the mixed crystals of required sizes with desirable properties.

Acknowledgements

The authors gratefully acknowledge Council of Scientific and Industrial Research (CSIR), Government of India for the financial support [Ref: no. 03 (1362/16/EMR-II].

References

[1] F. Brati, H. Rezagholipour Dizaji, Optical Quantum Electronics **48**, 432 (2016).
[2] Congting Sun, Dongfeng Xue, Optical Materials **36**(12), 1966 (2014).
[3] Jianxiu Zhang, Shufeng Zhang, Yicheng Wu, Jiyang Wang, Inorganic Chemistry **51**, 6682 (2012).
[4] J. Podder, Journal of Crystal Growth **237-239**, 70 (2002).
[5] K. Srinivasan, S. Anbukumar, P. Ramasamy, Journal of Crystal Growth **151**, 226 (1995).
[6] K. Srinivasan, P. Ramasany, A. Cantoni, G. Boceli, Materials Science and Engineering **B52**, 129 (1998).
[7] P. Shenoy, K. V. Bangera, G. K. Shivakumar, Crystal Research Technology **8**, 825 (2010).
[8] Xiue Ren, Dongli Xu, Donfeng Xue, Journal of Crystal Growth **310**, 2005 (2008).
[9] Fabrico Mendes Souza, Materials Research **20**, 532 (2017).
[10] P. Rajesh, P. Ramasamy, G. Bhagavannarayana, Journal of Crystal Growth **362**, 338 (2013).
[11] P. V. Dhanaraj, N. P. Rajesh, C. K. Mahadevan, G. Bhagavannarayana, Physica B **404**, 2503 (2009).
[12] P. Rajesh, P. Ramasamy, G. Bhagavannarayana, Journal of Crystal Growth **362**, 338 (2013).
[13] A. Silambarasan, P. Rajesh, P. Ramasamy, Journal of Crystal Growth **409**, 95 (2015).
[14] Keshra Sangwal, Crystal Engineering Communication **13**, 489 (2011).
[15] D. Jayalakshmi, R. Sankar, R. Jeyavel, J. Kumarl, Journal of Crystal Growth **276**, 243 (2005).
[16] Keshara Sangwal, Ewa Mielniczek Brzoska, Sylwia Baryska, Chemical Engineering and Research and Design **8762**, 00360-2 (2013).
[17] G. H. Sun, G. H. Zhang, X. Q. Wang, Z. H. Sun, D. Xu, Materials Chemistry and Physics **122**, 524 (2010).
[18] Senthilkumar Chandran, Rajesh Paulraj, P. Ramasamy, Journal of Crystal Growth **16**, 30686-8 (2016).
[19] M. S. Joshi, A. V. Antony, Journal of Crystal Growth **46**(1), 7 (1979).
[20] K. Sangwal, K. Wjcik, Crystal Research Technology **4**, 363 (2009).
[21] K. Sangwal, M. Szurg, Crystal Research and Technology **17**, 49 (1982).
[22] P. Rajesh, Urit Charoen In, Prapun Manyum, P. Ramasamy, Materials Research Bulletin **59**, 431 (2014).
[23] S. K. Chandran, R. Paulraj, P. Ramasamy, Molecular and Biomolecular Spectroscopy **51**, 432 (2015).
[24] R. N. Shaikh, M. D. Shirsat, P. M. Koinkar, S. S. Hussaini, Optics & Laser Technology **69**, 8 (2015).
[25] G. Babu Rao, P. Rajesh, P. Ramasamy, Materials Research Bulletin **60**, 709 (2014).
[26] Ying Wang, D. F. Eaton, Chem. Phys. Lett. **120**, 44 (1985).
[27] Qiu Feng, Xiang Jinzhong, Kong Jincheng, Yu Lianjie, Kong Lingde, Wang Guanghur, Li Xiongjun, Yang Lilli, Li Cong, Ji Rongbin, Journal of Semiconductors **32**, 033004 (2011).
[28] Senthilkumar Chandran, R. Jagan, Rajesh Paulraj, P. Ramasamy, Journal of Solid State Chemistry **230**, 135 (2015).

*Corresponding author: rajeshp@ssn.edu.in